Science of the Total Environment 765 (2021) 142737

Contents lists available at ScienceDirect

Science of the Total Environment

journal homepage: www.elsevier.com/locate/scitotenv

Old forests and old carbon: A case study on the stand dynamics and longevity of aboveground carbon

Dario Martin-Benito [a,*], Neil Pederson [b], Macarena Férriz [a], Guillermo Gea-Izquierdo [a]

[a] Forest Research Center INIA-CIFOR, Madrid, Spain
[b] Harvard Forest, Harvard University, Petersham, MA, USA

HIGHLIGHTS

- Old-growth forests are essential to understand natural forest dynamics, but are rare in Europe.
- Combining inventory and tree-ring analysis informs dynamics and long-term carbon storage.
- Small gaps and constant recruitment dominated dynamics in an old-growth oak forest.
- Carbon stored in above ground biomass for centuries with trees >400 years old.
- Tree longevity and low-intensity disturbance regimes resulted in long turnover times.

GRAPHICAL ABSTRACT

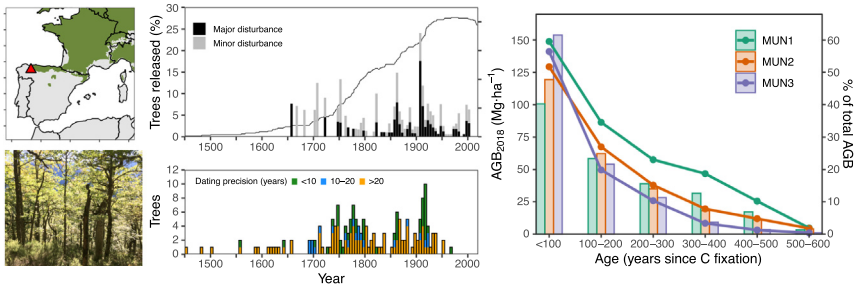

ARTICLE INFO

Article history:
Received 21 July 2020
Received in revised form 17 September 2020
Accepted 22 September 2020
Available online 8 October 2020

Editor: Elena Paoletti

Keywords:
Above ground biomass
Carbon age
Dendroecology
Forest dynamics
Sessile oak
Carbon turnover time

ABSTRACT

Most information on the ecology of oak-dominated forests in Europe comes from forests altered for centuries because remnants of old-growth forests are rare. Disturbance and recruitment regimes in old-growth forests provide information on forest dynamics and their effects on long-term carbon storage. In an old-growth *Quercus petraea* forest in northwestern Spain, we inventoried three plots and extracted cores from 166 live and dead trees across canopy classes (DBH ≥ 5 cm). We reconstructed disturbance dynamics for the last 500 years from tree-ring widths. We also reconstructed past dynamics of above ground biomass (AGB) and recent AGB accumulation rates at stand level using allometric equations. From these data, we present a new tree-ring-based approach to estimate the age of carbon stored in AGB. The oldest tree was at least 568 years, making it the oldest known precisely-dated oak to date and one of the oldest broadleaved trees in the Northern Hemisphere. All plots contained trees over 400 years old. The disturbance regime was dominated by small, frequent releases with just a few more intense disturbances that affected ≤20% of trees. Oak recruitment was variable but rather continuous for 500 years. Carbon turnover times ranged between 153 and 229 years and mean carbon ages between 108 and 167 years. Over 50% of AGB (150 Mg·ha^{-1}) persisted ≥100 years and up to 21% of AGB (77 Mg·ha^{-1}) ≥300 years. Low disturbance rates and low productivity maintained current canopy oak dominance. Absence of management or stand-replacing disturbances over the last 500 years resulted in high forest stability, long carbon turnover times and long mean carbon ages. Observed dynamics and the absence of shade-tolerant species suggest that oak dominance could continue in the future. Our estimations of long-term carbon storage at centennial scales in unmanaged old-growth forests highlights the importance of management and natural disturbances for the global carbon cycle.

* Corresponding author.
E-mail address: dmartin@inia.es (D. Martin-Benito).

https://doi.org/10.1016/j.scitotenv.2020.142737
0048-9697/

1. Introduction

Disturbances shape forest structure and developmental pathways (Bormann and Likens, 1979) and play a major role on biomass accumulation rates and storage. Growth rates, disturbance dynamics and mortality influence carbon fixation and turnover (Pugh et al., 2019). Intense or stand replacing disturbances generally reduce carbon stocks and reset stands back to younger stages, while small but frequent disturbances (e.g. gap dynamics) induce lower biomass declines but higher developmental variability (Bormann and Likens, 1979; Gough et al., 2016). Under climate change scenarios where disturbances are projected to increase (Seidl et al., 2017), it is important to define the baseline of disturbance rates or regimes for different forest types. Forest management is designed in part to mimic natural disturbances while optimizing sustainable productivity and other ecosystem services (Pretzsch, 2009). Management alters elements of natural forest dynamics such as regeneration, mortality, biomass accumulation, and species composition (Attiwill, 1994) in ways that may persist for decades or centuries.

The long history of intense forest management and land-use in Europe has made old-growth forests rare, particularly in Western Europe (Sabatini et al., 2018). Here, most hardwood forests, and, in particular, temperate deciduous oak forests (*Quercus petraea* (Matt) Liebl. and *Q. robur* L.) were converted into agricultural land, managed for timber or firewood or pollarded to allow grazing (Rozas, 2004; Bobiec et al., 2018). Thus, despite the extensive potential distribution area of these European oak species, old-growth forests or forests with little or no human influence with oaks as major species are very rare (Di Filippo et al., 2015). However, there still exist some rather large examples of old-growth tracts almost completely dominated by oak. Among them, the *Quercus petraea* forest of Muniellos Reserve in northwest Spain is regarded as one of the most extensive oak-dominated forests in Europe. Despite timber exploitation between the late 18th Century and 1973 (Torrente, 2000; Alvarez, 2002), parts of the reserve have been spared from logging and are considered to maintain a high degree of naturalness (Fernández Prieto and Sánchez, 1992). Notably, the Muniellos Reserve is home to endangered fauna like Cantabrian capercaillie (*Tetrao urogallus cantabricus* Castroviejo) and brown bear (*Ursus arctos* L.). As a whole, Muniellos offers a great potential to investigate forest dynamics and structure in unmanaged old-growth stands and their influence on forest development and the carbon cycle.

Natural disturbance regimes of forests in which oaks are important components have been described for different parts of the world by means of repeated inventories (Masaki et al., 1999; Brzeziecki et al., 2020) and dendroecological techniques (Abrams et al., 1997; Ruffner and Abrams, 1998; Rozas, 2004; Hart et al., 2012; Altman et al., 2016; Petritan et al., 2017; Heeter et al., 2019). The deeper time scale of dendroecological methods allows to reconstruct the frequency and magnitude of disturbance and recruitment events. Most of these forests are experiencing a general loss of oak dominance towards more shade tolerant species e.g. *Fagus sylvatica* L. in Europe (Petritan et al., 2017) or *Acer rubrum* L. in Eastern North America (Abrams et al., 1997) due to low rates of oak regeneration (McEwan et al., 2011). In Europe, the distribution and ecological ranges of *Q. petraea* and *Q. robur* largely overlap with those of *F. sylvatica*. Both oaks and beech form mixed forests where oaks are an important component of mid stages in the successional development (Petritan et al., 2017) because of their lower shade tolerance (Aranda et al., 2000). In many cases, later stages of forest development tend towards increasing beech dominance unless oak regeneration is favored by harvesting or fire (Bobiec, 2012; Saniga et al., 2014). Reduced frequencies of disturbances such as fire (Abrams, 1992) or other human influences (Bobiec et al., 2018; Brzeziecki et al., 2020) reduce the size of gaps required for oak regeneration while creating the closed-canopy conditions favoring shade-tolerant species. However, oaks generally have higher drought tolerance than those of shade-tolerant species, which allows them to thrive in marginal lands with lower soil water retention or poorer soils (Aranda et al., 2000; Cavin et al., 2013). In northwest Spain, where *Fagus sylvatica* became a common species only ca 3000 years cal BP, oak forests have constituted the dominant vegetation since the early Holocene (Kaal et al., 2011). Disturbance and recruitment dynamics in oak-dominated old-growth forests in Europe have rarely been analyzed (but see e.g. Rozas, 2004, Petritan et al., 2017).

Old-growth forests store large amounts of carbon in aboveground and soil biomass (Keith et al., 2009). Although, they have generally been considered carbon neutral, their capacity to fix and store carbon may have been underestimated (Carey et al., 2001) as positive carbon accumulations are reported even at very old ages (Luyssaert et al., 2008). In fact, fully stocked old-growth temperate forests may store the largest amounts of carbon per unit area among terrestrial ecosystems (Luyssaert et al., 2008; Keith et al., 2009). Much of this carbon could be stored for centuries. The time that fixed carbon remains in the forest and the age of carbon since its time of entry into the system (Sierra et al., 2017) likely depends upon many factors, including productivity, structure, disturbance regime, and species composition. Old-growth forests are unique systems towards understanding natural stand dynamics and carbon accumulation in the absence of direct human influence (Foster et al., 1996).

Different estimators are used to approximate how effective ecosystems are to retain carbon and how long that carbon is fixed. Carbon residence times or turnover times have commonly been estimated from different types of data as the ratio of carbon stock and either the rate of carbon accumulation or the rate of carbon loss (Sierra et al., 2017). Carbon residence time commonly increases with increasing biomass stock and decreases with forest productivity (Keeling and Phillips, 2007). Young productive forests may have higher annual productivities than old-growth forests, but have shorter turnover times. However, carbon turnover times can differ greatly from the amount of time that carbon resides fixed in forest biomass (system age) if certain assumptions are not met, particularly the steady state of the system (Sierra et al., 2017). Because fixed carbon in wood represents the largest amount of forest aboveground biomass (AGB), analyzing the ages of AGB based on tree-ring techniques, where each growth ring is assigned an exact calendar date, has the potential to offer a precise approach to carbon age estimation in forests. Such dendrochronological approach would be informative both in old-growth forest landscapes subject to natural disturbances as well as in managed or younger secondary forests. The precisely-dated information drawn from the growth rings and ecological events would add a deep temporal dimension to total AGB stock. To our knowledge, this approach has not been used before.

The aim of this study was to analyze natural forest dynamics in a *Quercus petraea* old-growth tract and climate influence on stand level AGB and discuss how they affect carbon dynamics, including carbon turnover time and mean carbon age. Here, we use a combination of dendroecological techniques and detailed forest inventory to describe the structure of these rare old-growth systems and reconstruct the stand dynamics of disturbances and recruitment through the last five centuries. We also present a new approach to estimate the age of aboveground carbon that has been accumulated through time and is currently present in the forest. Our findings will contribute to a more complete understanding of the dynamics and ecology of oak-dominated forests as well as the patterns and processes that have shaped their structure and species composition.

2. Material and methods

2.1. Study area and field methods

Our study area was within the UNESCO Muniellos Biosphere Reserve (ca. 5500 ha) in the western Cantabrian Mountains of Spain (43.02 N, 6.69 W, Fig. 1). These forests belong to the acidophilous oakwood types (European Environment Agency, 2006) dominated by *Quercus*

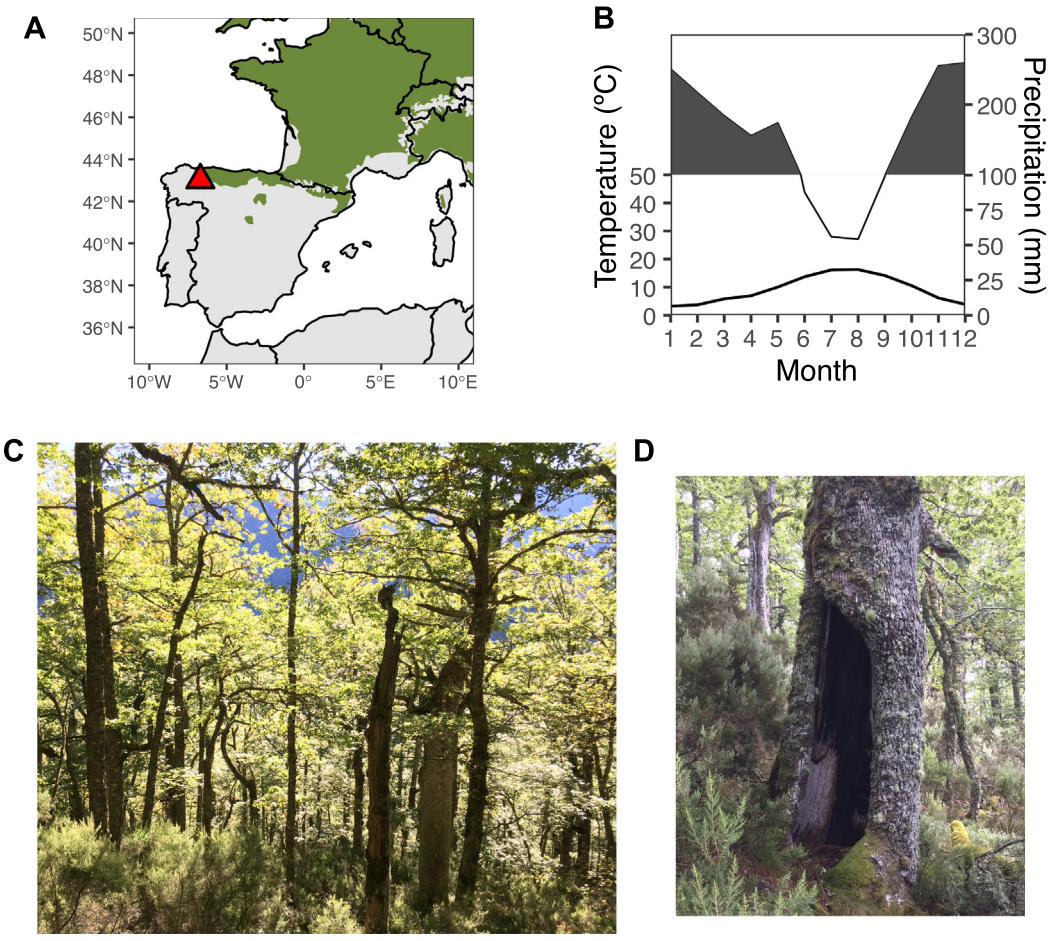

Fig. 1. Location of study site and climate diagram. A) Location of the study site in NW Spain (triangle) and distribution area of *Quercus petraea* in western Europe (green shade) (source: EUFORGEN, www.euforgen.org). B) Climate diagram showing temperature and precipitation for the study site with dark grey shade showing mean monthly precipitation exceeding 100 mm. Panels C (MUN3) and D (MUN1) show the general structure of our study old-growth forest.

petraea and have a dense shrub layer of *Erica arborea* L., *Vaccinium myrtillus* L. and a herb layer with *Deschampsia flexuosa* (L.) Trin. and *Luzula sylvatica* (Huds.) Gaudin (Sabatini et al., 2014). Soils are shallow, umbric regosols, over siliceous substrate (quartzite, schists and slates) with variable organic horizon (Díaz-Maroto et al., 2011), abundance of exposed rocks, and have low water holding capacities (Sabatini et al., 2014). Our study forest was located on a southwest slope at 1000–1100 m a.s.l. and corresponds with the mesophilous sessile oak forest type, which cover most of the reserve (Fernández Prieto and Sánchez, 1992). The reserve is close to the Western limits of *Quercus petraea* distribution (Fig. 1).

Abundant precipitation allows for the development of dense forests, despite the shallow soils. Monthly precipitation and temperature were available from several weather stations, including one inside the reserve at 670 m a.s.l., covering much of the period 1967–2019. We used data from all stations to estimate lapse rates for precipitation and temperature and complete gaps in the reserve station. We extended this local climate data to the period 1950–2018 using the closest *E*-OBS v15 grid-point (Haylock et al., 2008). We also estimated the drought index Standardised Precipitation-Evapotranspiration Index (SPEI) for periods between 1 and 12 moths (Vicente-Serrano et al., 2010). Climate is temperate oceanic with annual precipitation of 1970 mm and mean temperature of 9.23 °C (Fig. 1). A short dry period may develop during the summer. Mean annual temperature increased by 0.12 °C·decade^{-1} ($p = 0.002$) and precipitation by 38.8 mm·decade^{-1} ($p = 0.039$) between 1950 and 2018 (Appendix A: Fig. A.1).

We identified a stand with old-growth characteristics (Fig. 1) following the criteria established for old-growth oak forests in eastern north America (Stahle and Chaney, 1994) and where trees showed characteristics of old trees in temperate forests (Pederson, 2010). We estimate the studied old-growth stand to be about 100 ha. Here, we randomly established three circular plots 60 m in diameter (~2827 m^2) labeled MUN1, MUN2, and MUN3. Each plot contained three concentric subplots 5 m, 20 m, and 30 m in radius with thresholds of minimum diameter at breast height (DBH) for trees to be selected of 5 cm, 15 cm, and 40 cm, respectively (Martin-Benito et al., 2020). For each tree, we measured DBH, height, and tree position. Canopy position was recorded as dominant, codominant, intermediate, or suppressed based on the amount of light reaching the crown (Oliver and Larson, 1996). We extracted 1–3 cores from all living trees and all dead trees solid enough to be cored. The goal of the sampling design is to increase the number of large trees while including some representation of smaller trees. Analyses of designs similar to ours indicate this approach can result in accurate estimates of annual productivity (Xu et al., 2019). Importantly, our design allows to develop growth chronologies not only at tree level but also at the stand level (e.g. growth per surface unit area) which includes tree growth and abundance (Dye et al., 2016; Martin-Benito et al., 2020), and overcome biases of studies sampling only dominant individuals (big-tree selection bias) or live trees (pre-death suppression bias) (Bowman et al., 2013). By sampling across a representative range of DBH, this design also reduces the false negative bias in disturbance detections associated with sampling just dominant trees (McEwan

et al., 2014). Although fire-scarred trees were observed in (six trees) and around the plots (Appendix A: Fig. A.2), strict protection in the reserve prohibits the extraction of wedge samples to precisely date fire scars using tree rings.

2.2. Dendrochronological methods and disturbance analysis

Cores were sanded until growth rings became clearly visible. Rings were visually crossdated, measured with a 0.01 mm precision with a LINTAB measuring station (Rinn, 2003) and then statistically verified with COFECHA (Holmes, 1983). Ring widths for the same tree (1–3 cores per tree) were averaged for each calendar year. Past tree DBH and basal area increments (BAI) were estimated by subtracting mean annual growth from field-measured DBH. For trees where pith was not reached, we estimated the number of rings to the pith with a geometrical approach based on inner rings curvature and early growth (Duncan, 1989).

As indicators of past disturbances, we analyzed tree releases from competition based on ring-width series with the radial growth averaging method (Lorimer and Frelich, 1989). For this method, growth changes (GC_i) between 10 years prior ($M1_i$) and 10 years after ($M2_i$) any given year i were estimated as $GC_i = \frac{M2_i - M1_i}{M1_i} \times 100$ where $M1_i = \overline{\sum_{j=i-10}^{j=i-1} RW_j}$ represents mean growth 10 years prior and $M2_i = \overline{\sum_{j=i}^{j=i+9} RW_j}$ mean growth 10 years following year i. Disturbances are characterised as sudden and sustained increases in growth. We considered moderate growth releases those with 50 % ≤ GC_i < 100% and major releases when GC_i ≥ 100%. For disturbance analysis, we used packages dplR (Bunn, 2008) and TRADER (Altman et al., 2014) in R (R Core Team, 2019). Disturbance intensity was expressed as the percentage of trees recording a disturbance.

2.3. Above ground biomass

We estimated woody above ground biomass (AGB) at the time of inventory from allometric equations based on tree height and DBH for oaks in Northern Spain which include all woody fractions from branches with a diameter < 2 cm to the entire tree stem (Manrique González et al., 2017). Our plots were not designed to accurately estimate deadwood volumes, because only large pieces of deadwood lying or standing (snag) or solid enough to be cored were considered in our protocol and sampled. We note, however, that no large pieces of lying deadwood were present in the sampled plots and only snags were measured and sampled.

We reconstructed AGB back in time for each tree from reconstructed DBH based on tree-ring widths (Graumlich et al., 1989; Davis et al., 2009; Dye et al., 2016). For trees whose pith was not reached, we completed ring widths for missing years with the average annual ring width of trees within the same 5-cm DBH class. Because past tree height could not be reconstructed, we used allometric equations for wood volume of *Q. petraea* that only required DBH (Vallet et al., 2006) and estimated AGB applying a constant wood density of 0.63 $Mg \cdot m^3$ for the species (Castaño-Santamaría and Bravo, 2012). We estimated the AGB increments (AGBI) as the per hectare sum of annual individual tree AGB increments of all trees, which would be roughly equivalent to aboveground woody net primary productivity (ANPP; Graumlich et al., 1989, Davis et al., 2009, Dye et al., 2016).

Allometric equations used to estimate woody AGB or AGB increments (AGBI) from annual radial growth are an important source of uncertainty. Allometric equations that include DBH and tree height are usually more accurate than those based only on DBH (Cienciala et al., 2008). Height growth cannot be readily reconstructed back in time and using DBH: height relationships would add further uncertainty particularly for old-growth forests which may follow different DBH: height relationships than younger or more productive forests. Additionally, the high interannual variability in tree-ring width may only be partially mirrored by similar variability in AGB increments at the tree and stand level (Klesse et al., 2016). However, previous studies using similar approaches show AGB and AGBI from repeated measurement in permanent plot data are accurately represented by AGB from tree rings for periods of 40 years or longer (Dye et al., 2016; Klesse et al., 2016).

Carbon sequestered in AGB can stay in the forest for variable periods of time. By definition, young forests would only contain recently-fixed woody AGB. In contrast, AGB in old forests may have a broad range of ages depending on disturbance rates, stand structure, tree ages, and growth rates. We calculated two complementary time metrics commonly used to describe the capacity of systems to store carbon: turnover time (also referred to as residence time) and system age (Sierra et al., 2017). We estimated turnover time of current AGB (tr, in years) in each plot using a steady state approach (Berner et al., 2017) as $tr_{AGB} = AGB_{2018}/AGBI_{50y}$ i.e., the ratio between AGB stock (AGB_{2018}) and mean AGB increments for the last 50 years (forest growth, $AGBI_{50y}$). This approach assumes constant growth rates and little or no variation in carbon stock over time (steady state). For consistency, AGB_{2018} and $AGBI_{50y}$ were estimated with the same allometric equations that only required DBH (Vallet et al., 2006). We chose 50 years for $AGBI_{50y}$ because AGBI was stable over that period (see results), as suggested for other temperate forests (Dye et al., 2016). Using shorter time periods (20, 30 and 40 years) generated similar results. For comparison to our findings, we estimated tr with AGB and AGBI data reported in Keeling and Phillips (2007) from other 54 temperate forests in the world.

To estimate biomass system age, we present a new approach based on AGB reconstructed from tree rings. Cross-dated time series of growth, a standard practice in dendrochronology, allow for the identification when carbon was fixed into biomass with annual precision. Thus, we defined system age as the age of biomass in forest trees, i.e. the age of carbon in all woody fractions in the stand at the time of sampling in 2018. By definition, these estimates do not include biomass not retained (i.e. fixed but lost before 2018) but do include present deadwood that could be cored. For the multidecadal time-scales on which we focused here, the potential effect of the age of non-structural carbohydrates used for growth was considered negligible (Carbone et al., 2013). We present results on carbon age distribution binned by 100-year age classes. We also estimated a AGB-weighted mean age of AGB (mean carbon age, MCA) as $MCA = \frac{\sum_{i}^{n} \tau_i \cdot AGBI_i}{\sum_{i}^{n} AGBI_i}$ where $AGBI_i$ is AGB increment for age i and n is the maximum age of AGB and τ_i the age of AGBI. We note that tr and MCA are identical for AGB and the carbon contained in AGB. This new approach relaxes the assumptions of steady state and constant growth to complement estimates of turnover times.

2.4. Climate-biomass relationships

To elucidate how climate affects tree and stand growth, we also used correlation analysis of biomass increments (AGBI) with monthly and seasonal climate for the period 1950–2018. For stand level and canopy position level analysis, we used the approach described by Teets et al. (2018). Briefly, we summed AGBI from all trees in each category and plot (stand, canopy position) and then averaged for the three plots as dependent variable. We considered climate variables either monthly or averaged seasonally (DJF, MAM, JJA, SON), from previous spring to current fall. First, we selected all variables with significant correlations ($p < 0.05$) with each AGBI chronology. Then, we fitted generalized least squares (GLS) regression models between AGBI and preselected climate covariates with a stepwise selection of variables with significance set at $p < 0.05$ using package *nlme* (Pinheiro et al., 2019) in R (R Core Team, 2019). Models accounted for first order temporal autocorrelation by including an autoregressive error term. To avoid collinearity between independent variables, we removed all variables with variance inflation factor (VIF) above 4.

Table 1
Summary of stand variables for the study plots.

Plot	Density[a] (trees·ha^{-1})	Basal area[a] (m^2·ha^{-1})	Total AGB[a] (Mg·ha^{-1})	Deadwood AGB[b] (Mg·ha^{-1})	Volume* (m^3·ha^{-1})	Deadwood volume* (m^3·ha^{-1})	DBH$_s$ (cm)		DBH$_w$ (cm)	Height$_s$ (m)		Height$_w$ (m)
							Mean (sd)	Range	Mean (sd)	Mean (sd)	Range	Mean (sd)
MUN1	158.3	54.8	399.0	17.3	714.4	36.1	64.35 (25.10)	21.2–111.0	61.00 (26.28)	17.33 (3.71)	9.0–25.6	16.94 (3.78)
MUN2	211.3	45.0	252.0	4.2	499.7	13.5	50.29 (17.80)	25.5–118.5	48.85 (18.01)	14.90 (4.77)	6.1–24.2	14.69 (4.94)
MUN3	670.2	44.9	211.3	3.5	432.1	10.1	41.88 (14.59)	9.2–107.0	23.50 (17.36)	11.65 (4.18)	2.5–27.7	8.28 (4.35)
Stand	346.6	48.2	287.4	8.4	548.7	19.0	50.11 (20.55)	9.2–118.5	34.36 (24.32)	14.10 (4.84)	2.5–27.7	10.90 (4.67)

a, of trees DBH ≥ 5 cm per hectare.
b, only standing dead trees (snags) were found.
AGB estimated with equations requiring DBH and tree height (Manrique-González et al., 2017).
*, including main stem, branches and twigs.
s, means and SD for all sampled trees; w, means and SD weighted by estimated presence per hectare.

3. Results

3.1. Forest structure and biomass

The forest was dominated by *Q. petraea* with stand densities of trees with DBH ≥ 5 cm between 158 and 670 trees·ha^{-1} (mean 347 trees·ha^{-1}) (Table 1). Sampled trees averaged a DBH of 50.1 cm (range 9.2 cm - 118.5 cm) and height of 14.1 m (2.5–27.7 m). Most values of tree height-to-DBH ratio (slenderness) were below 50 (Appendix A: Fig. A.3). The diameter distribution (Fig. 2) for the forest showed a decrease in abundance from small to medium trees (DBH ≤ 20 cm, 146 trees·ha^{-1}) towards the less frequent large trees (DBH ≥ 70 cm, 37 trees·ha^{-1}). The three plots differed in the density of small to medium trees (DBH ≤20 cm), more abundant in MUN2 and absent in MUN1 (Appendix A: Fig. A.4). In contrast, large trees were more abundant in MUN1.

Differences in the DBH distribution between plots resulted in large differences in terms of AGB and volume (Table 1, Fig. 2B). Large trees (DBH ≥ 70 cm) stored on average 50% of total AGB. MUN1 with the lowest stem density, but highest density of large trees (67.2 trees·ha^{-1}), had an AGB of 399 Mg·ha^{-1}. In contrast, the densest plot MUN3 had an AGB of 211 Mg·ha^{-1}. Volume followed the same pattern with the highest value in MUN1 (714 m^3·ha^{-1}) and lowest in MUN3 (432 m^3·ha^{-1}). Deadwood AGB averaged 8.4 Mg·ha^{-1}, less than 3% of total AGB, and roughly equivalent to 19.0 m^3·ha^{-1} and 53 trees·ha^{-1}. Most snags were in the smallest DBH class, with the largest one in the 55-cm DBH class.

3.2. Disturbance dynamics and recruitment

According to our release detection analysis, our study forest experienced frequent low-intensity disturbances for most of the last 400 years, i.e. since 1620 when sample size was above 10 trees (Fig. 3). At the stand level, most major releases affected less than 10% of trees during any 5-year period. The exception was during the 1905–1915 disturbance when around 20% of trees present recorded a major growth release. This event was mostly due to more disturbance in MUN2 and MUN3 (Appendix A: Fig. A.5). Smaller disturbances that affected 20% of trees, occurred around 1860–1870. For the most reliable period after 1700 (replication >20 trees), almost every decade experienced a disturbance. Our sampling across a wide range of DBH and canopy classes allowed to identify a most recent release event in 1995–2005.

Tree recruitment generally lagged disturbances by 5–10 years, particularly the larger ones in 1860–70 and 1905–1915. Over the last 200 years, two periods of low regeneration occurred around 1830–1850 and the late 1890s. These recruitment dynamics shaped age distributions at the stand level (Fig. 3c). The oldest tree sampled was at least 568 years old (i.e., 568 rings dated in the core back to year 1451), but because its longest core was missing 6.9 cm to the pith, we estimated it could be around 620 years old 1.3 m above the ground. The oldest tree in the youngest plot had 398 rings at coring height, but its longest core was missing 14.9 cm, so it is safe to assume that all plots had trees over 400 years old. The most abundant trees in the forest with DBH ≥ 5 cm were 90–105 years old (115 trees· ha^{-1}, 38% of trees), originating after the disturbance event in 1905–1915. This cohort was particularly abundant in MUN3 (58% of trees). Trees 200–330 years old were the second most abundant cohort (94 trees· ha^{-1}, 31% of trees). Trees older than 330 years of age made up 6% of trees (19 trees·ha^{-1}). There were 16 trees·ha^{-1}, roughly 5% of all trees with DBH ≥ 5 cm, that were also <90 years old.

3.3. Forest growth and carbon age

The sum of annual AGB growth of live and dead trees (AGBI) present at time of sampling (autumn 2018) averaged 1.47 ±

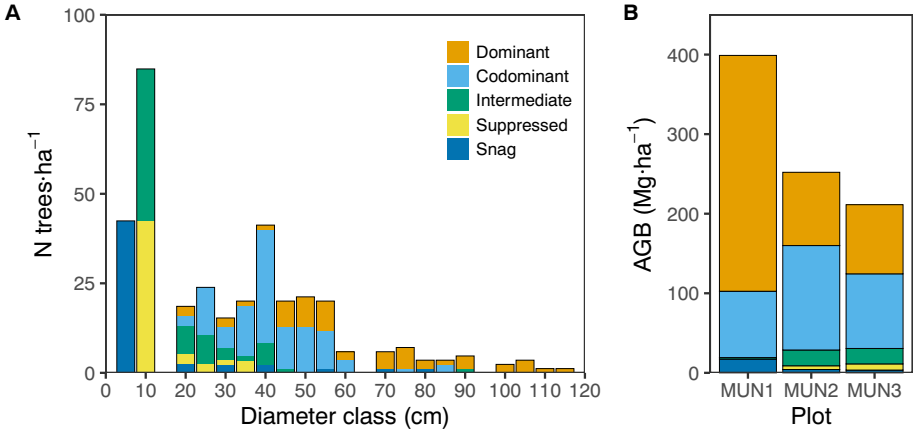

Fig. 2. Forest stand structure: A) Stand density per DBH class (5-cm classes) mean for three plots (data plotted at diameter class mid-points); B) Above ground biomass (AGB, Mg·ha^{-1}) per plot and tree canopy classes.

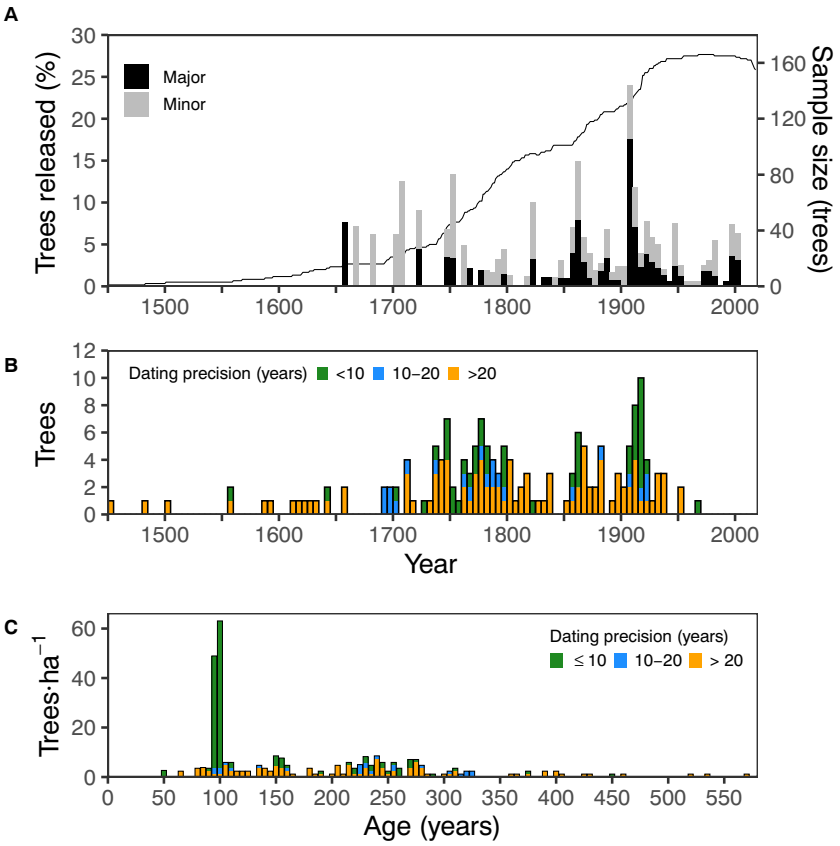

Fig. 3. Forest disturbance dynamics as A) release chronology for the three plots combined expressed as percentage of trees released per 5-year since 1468 by release type (minor, increases in growth >50% and < 100%; major, growth increases ≥ 100%). Total bar height represents cumulative % of trees recording minor and major releases. Disturbance chronology truncated to sample depth above 10 trees. B) Recruitment dates of trees sampled and dated; green shows trees for which pith was reached (i.e. complete ages) or estimated to be within 10 years, blue those trees between 10 and 20 years away from the pith, while orange shows trees for which the pith was estimated to be more than 20 rings away; C) age structure (trees per hectare) including the three sampled plots with same colour scheme as panel B.

0.29 $Mg \cdot ha^{-1} \cdot year^{-1}$ over the last 50 years (Table 2). Despite high interannual variability, these medium-term growth rates remained relatively stable since at least 1950 (Fig. 4). Most annual growth at the stand level (89% AGBI) was due to dominant and codominant trees. Intermediate and suppressed trees represented 9.9% of stand AGBI owing to their higher relative abundance in MUN2 and MUN3. Longer time scales showed differing inter-plot growth patterns of trees present in 2018 (Appendix A: Fig. A.6). While MUN1 stand-level growth rates (AGBI) increased mostly uniformly over time, MUN2 growth rates started increasing mostly after the early 1700s with most growth occurring after 1900. Growth in MUN3 was a mixture of both patterns. Growth increases in MUN2 and MUN3 after 1900 coincided with growth releases detected in those plots, but were also influenced by increased tree recruitment post-disturbance. Since 1950, the forest showed three multi-year periods of declining woody biomass growth centered around 1977, 1995 and 2017. Average AGB increments dropped below 1 $Mg \cdot ha^{-1} \cdot year^{-1}$ during only two years since 1950: in 1995 (0.89 $Mg \cdot ha^{-1} \cdot year^{-1}$) and 2017 (0.83 $Mg \cdot ha^{-1} \cdot year^{-1}$).

The age of above ground biomass (AGB) differed between plots (Fig. 5). All plots showed similar values of young AGB (<100 years),

Table 2
Summary statistics for plot and stand growth chronologies and age characteristics. All sampled trees from different crown classes are included.

Plot	Trees (cores)	Rbar[a]	Time span	Age_s (years)		Age_w (years)	BAI_{50y} ($cm^2 \cdot ha^{-1} \cdot year^{-1}$)	Total AGB[a] ($Mg \cdot ha^{-1}$)*	$AGBI_{50y}$ ($Mg \cdot ha^{-1} \cdot year^{-1}$)*	tr (years)	MCA (years)
				Mean (sd)	range	Mean (sd)	Mean (sd)		Mean (sd)		
MUN1	40 (65)	0.479	1483–2018	238.5 (140.6)	51–536	228.2 (138.1)	1993.3 (358.3)	365	1.59 (0.28)	229	167
MUN2	56 (84)	0.482	1661–2018	218.2 (65.8)	79–398	216.2 (65.6)	1895.3 (326.1)	269	1.32 (0.22)	203	143
MUN3	70 (97)	0.479	1451–2018	191.9 (94.1)	79–568	141.4 (79.3)	2546.9 (451.6)	230	1.50 (0.28)	153	108
Stand	166 (266)	0.481	1451–2018	212.0 (100.8)	51–568	173.8 (97.7)	2144.8 (476.3)	321	1.47 (0.29)	195	144

a, mean series correlation with master chronology;
s, means and SD for all sampled trees; w, means and SD weighted by estimated presence per hectare.
*, estimated with allometric equations requiring only DBH (Vallet et al., 2006).
tr, turnover time.
MCA, Carbon-weighted mean carbon age.

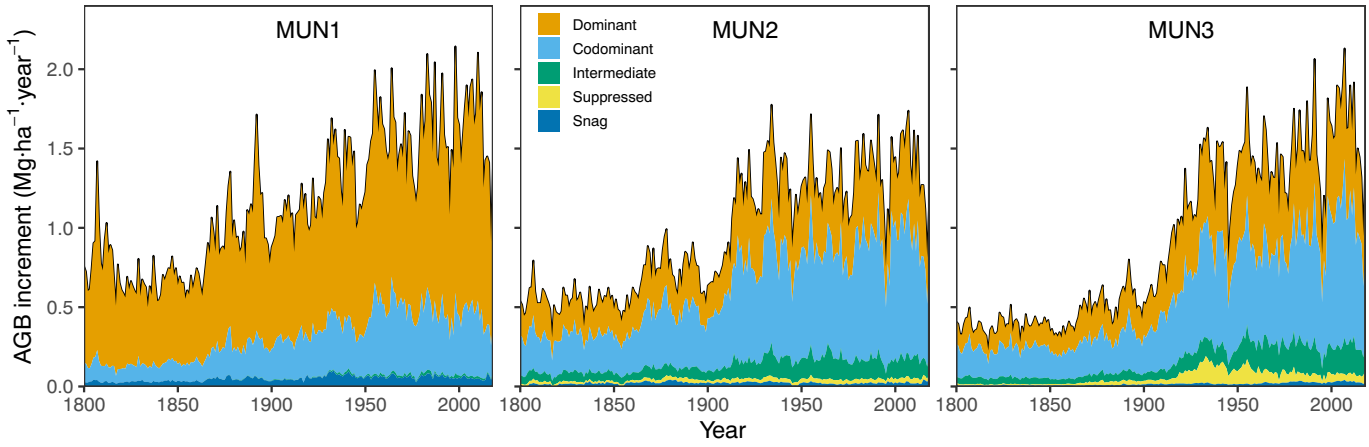

Fig. 4. Total aboveground biomass (AGB) increment per hectare 1800–2018 of trees present at time of sampling (2018). Different areas represent AGB increments for tree canopy positions. Areas for different canopy class are stacked and total AGB increment per plot is shown with a thin black line. The full temporal extent of the data is shown in Appendix S1: Fig. S6.

ranging between 129 Mg·ha^{-1} in MUN2 and 149 Mg·ha^{-1} in MUN1, although that represented 40% in MUN1 and 62% in MUN3. Considering its age structure, it follows that older AGB fractions were lower in MUN3 than the other two plots. There was less AGB in the 100–200 years range (50 Mg·ha^{-1}; 22%) in MUN3 than in MUN1 (86 Mg·ha^{-1}) and MUN 2 (68 Mg·ha^{-1}). Very old AGB (carbon >300 years old) ranged between 77 Mg·ha^{-1} (21%) in MUN1 and 13 Mg·ha^{-1} (5.5%) in MUN3. Overall, very old AGB composed an average of 42 Mg·ha^{-1} over the landscape. Mean carbon age (MCA) in the plots ranged between 108 and 167 years with a stand average of 144 years.

We estimated an average carbon turnover time (*tr*; $AGB_{2018}/AGBI_{50y}$) of 195 years for the forest, with *tr* in the three plots ranging between 153 years and 229 years (Table 2). These turnover times were above the 90th percentile of a global database of 54 other temperate forests (Fig. 6). Using mean AGB increments for 20, 30 or 40 years resulted in similar *tr* (141–148 years to 223–228 years; results not shown).

3.4. Climate biomass-growth relationships

Our multivariate linear growth models indicated that climate accounted for 31% of the total AGB increment interannual variance at the stand level (Table 3; Appendix A: Fig. A.7). Variance explained by the models ranged between 14% for suppressed trees and 33% for

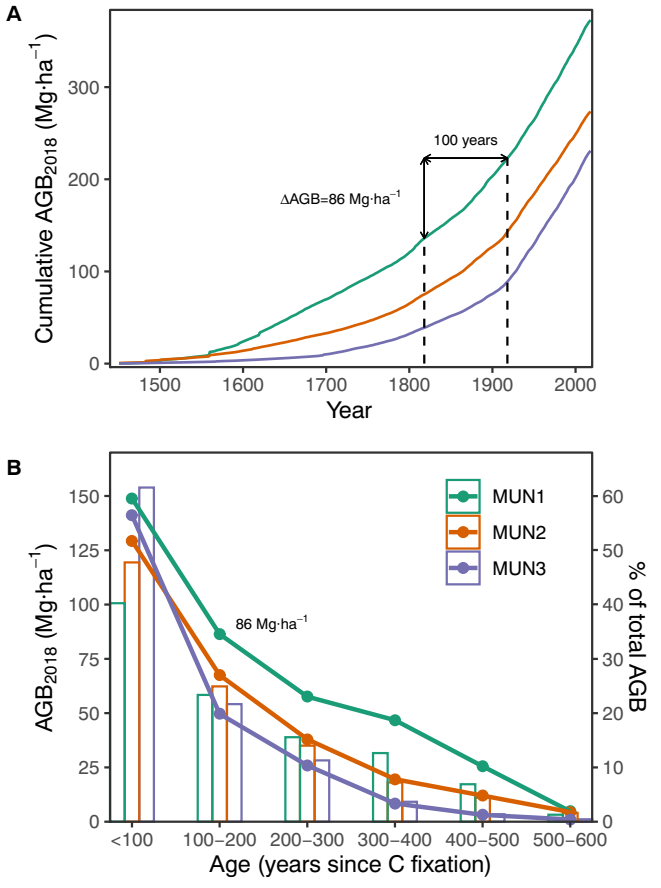

Fig. 5. Cumulative woody above ground biomass (AGB_{2018}) present at time of sampling (Autumn 2018). A) AGB_{2018} through time for each plot. B) Age of AGB fixed present at time of sampling in each plot (lines, left axis) and percentage of AGB in each 100-year age class over total AGB_{2018} (columns, right axis). As an example of AGB_{2018} accumulated during different periods, the amount of AGB_{2018} fixed in plot MUN1 between 1818 and 1918 (86 Mg·ha^{-1}) is shown in panel A (vertical dashed lines). That AGB was 100–200 years old at time of sampling (panel B).

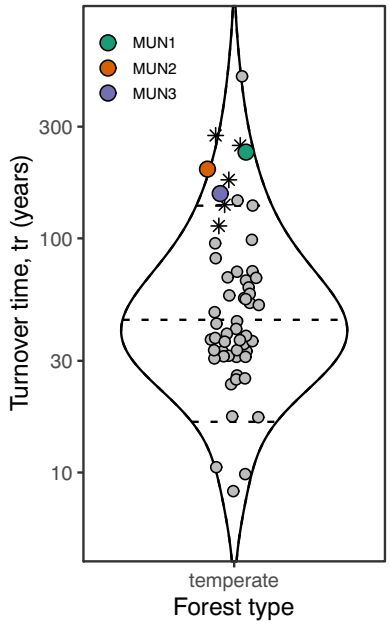

Fig. 6. Biomass turnover time (*tr*) in our three study plots (coloured circles) compared to *tr* from a global database of 54 temperate forests (grey circles and asterisks, violin plot) in Keeling and Phillips (2007). Asterisks represent sites considered outliers in Keeling and Phillips (2007). Dashed horizontal lines represent 10th, 50th, 90th percentiles. Note the logarithmic scale in the y-axis.

Table 3
Model selection for AGB increments for different canopy classes (mean of all plots) based on climate variables for the period 1950–2018. Stand level includes all canopy classes combined (mean of all plots). Snags were not used for this analysis due to low sample size.

Canopy level	Climate	Estimate	SE	t statistic	*p* value	df	pseudo R^2	RMSE	MAE	Bias
Stand	$SPEI12_{pJun}$	−0.0583	0.0215	−2.7085	0.0087	48	0.31	0.190	0.153	−0.0048
	$Precip_{DJF}$	−0.0012	0.0004	−3.1675	0.0024					
	$Tmean_{pSON}$	0.0680	0.0215	3.1649	0.0024					
Dominant	$SPEI6_{pSep}$	−0.0228	0.0098	−2.3407	0.0224	58	0.33	0.0895	0.072	−0.0020
	$Precip_{DJF}$	−0.0005	0.0002	−2.7316	0.0082					
	$Tmean_{pSON}$	0.0332	0.0101	3.2835	0.0017					
Codominant	$SPEI12_{pAug}$	−0.0266	0.0093	−2.8704	0.0056	50	0.28	0.0875	0.071	−0.0029
	$Precip_{DJF}$	−0.0005	0.0002	−2.9078	0.0050					
	$Tmean_{pSON}$	0.0325	0.0095	3.4314	0.0011					
Intermediate	$Tmean_{pSON}$	0.0044	0.0021	2.0647	0.0430	51	0.15	0.0201	0.015	−0.0002
	$SPEI12_{pJJA}$	−0.0053	0.0021	−2.5128	0.0145					
Suppressed	$Precip_{May}$	$-3.94 \cdot 10^{-5}$	$1.48 \cdot 10^{-5}$	−2.6659	0.0097	62	0.14	0.009	0.007	0.0002

DJF, December, January. February; SON, September, October, November.
p, denotes variables of the year previous to ring formation.
df, degrees of freedom.
SE, standard error.
pseudo R^2, correlation between observed AGBI and predicted values with corresponding model.
RMSE, root mean square error.
MAE, mean absolute error.

dominant trees. Among climate covariates, those of the year before tree ring formation were the most influential for stand-level and canopy-class level AGB increment. Winter precipitation ($Precip_{DJF}$) decreased AGB increment, whereas higher mean temperature of the previous fall ($Tmean_{pSON}$) enhanced it. Medium-term drought (6, 12 months) during the previous summer ($SPEI12_{pJun}$, $SPEI12_{pAug}$, $SPEI3_{pJJA}$) or early fall ($SPEI6_{pSep}$) increased AGB growth at stand level and in all canopy classes (Table 3).

4. Discussion

We identified patches of forest growing on steep slopes with the structural and age characteristics of old-growth forests, despite centuries of logging in the areas surrounding our study site (Alvarez, 2002). These forest patches likely developed under a natural dynamics regime that lead to a monospecific *Quercus petraea* forest with diverse ecosystem and age structures. Our study forest contains the oldest precisely-dated oak known to date and some of the oldest broadleaf deciduous trees in the Northern Hemisphere. The three oldest trees were at least 568 years, 536 and 518 years old, but we estimated that some of these trees could most likely be over 600 years. Oak ages reported for other parts of the world often show longevities over 400 years (Appendix B: Table B.1), but confirmed ages over 500 years, as opposed to estimated ages, are rare in part due to past land uses (Di Filippo et al., 2015) or high rates of stem decay which preclude precise tree-ring aging (Ranius et al., 2009). Recently, a live *Q. petraea* tree has been radiocarbon dated to be 934 ± 65 years old in Italy, suggesting that longevity of many tree species might be longer than has been documented to date (Piovesan et al., 2020). Including the ages reported here, northern Spain appears to hold some of the oldest reported precisely-dated ages for oaks in Europe, including 496 years for *Q. petraea* (Domínguez-Delmás et al., in review), *Q. robur* reaching 480–500 years (Rozas, 2004; Souto-Herrero et al., 2017), *Q. pyrenaica* estimated to be 502 years old based on 422 dated rings and early growth rates (Gea-Izquierdo and Cañellas, 2014), or the 509 years of *Q. faginea* Lam. (Domínguez-Delmás et al., in review). In California, while the oldest live *Q. douglasii* found was 462 years old, a dead *Q. douglasii* had 553 rings but was missing the innermost rings (Stahle et al., 2013). Within broadleaves, only a few *Fagus sylvatica* trees (622 years) (Piovesan et al., 2019) and *Nyssa sylvatica* Marsh. (679 years) (Sperduto et al., 2000) reached older ages. Considering the results from our census, where all plots included trees exceeding 400 years old, we expect that more trees of similar or older ages likely remain in the landscape. Old-growth forests with such abundance of old trees are scarcer than scattered old trees, which can be often found in human-transformed landscapes (Rozas, 2004; Drobyshev et al., 2013). In Muniellos, slow growth, low intensity disturbance, and the lack of human influence may have favored the abundance of long-lived oaks.

4.1. Disturbance regime

The disturbance regime identified in our old-growth forest from radial growth patterns reflects the high-frequency but low-severity disturbances of gap dynamics over the last 500 years. Disturbances were recorded in almost every decade since the late 1690s but no major disturbance affected more than 20% of the trees. Although no studies of long term disturbance dynamics in old-growth *Q. petraea* forest exist, such low rates of disturbance are not uncommon to some oak-dominated old-growth forests in North America (Cho and Boerner, 1995; Abrams et al., 1997; Heeter et al., 2019). However, the periods of largest disturbance identified (1860–70 and 1905–1915) coincide with two periods of logging activity in the reserve (Torrente, 2000; Alvarez, 2002). Thus, some effects of logging cannot be completely ruled out; precise information on logging dates and places were not available. Our results described a disturbance regime dominated by small canopy gaps. Small-scale canopy disturbances would be caused by the death of a single or a few trees, partial tree breakage or decline due to disease, repeated drought, or other factors (Manion, 1981) rather than large-scale synchronous disturbances like logging, wind-throw or crown fires (Runkle, 1985). Low tree slenderness and relatively open canopies in our study forest reduce the probability of large disturbances from agents like wind-throw compared to closed-canopy forests (Trotsiuk et al., 2016; Martin-Benito et al., 2020) because less slender trees have a lower risk of wind breakage (Jackson et al., 2019). In addition, tree external characteristics and ring patterns showed no signs of pollarding, common in many old oaks in northern Spain (Rozas, 2005), further evidencing the old-growth state of our study forest.

As a medium shade-tolerant species, *Q. petraea* seedlings commonly require high light availability to access the canopy or regenerate (Rodríguez-Calcerrada et al., 2008; Bobiec et al., 2018) and these light requirements increase with age (Annighofer et al., 2015). Under strong competition for light in mixed beech-oak forests, *Q. petraea* episodic regeneration generally follows disturbance (Petritan et al., 2017). We observed a similar peak in regeneration around 1925 following the larger disturbance around 1910 affecting 20% of the trees. Our results, however, showed continuous, but variable recruitment over the last

500 years and the absence of more shade-tolerant species. Strong dominance of deciduous oaks across large landscapes is uncommon in Europe or other temperate zones. Oak dominance is usually restricted to edaphic conditions with low water-retention capacity, steep slopes or southern aspects that exclude less drought-tolerant species (Stahle and Chaney, 1994; Abrams et al., 1997; Ruffner and Abrams, 1998; McEwan et al., 2014). Under these conditions in the northwestern Iberian peninsula, oak forests constitute the dominant vegetation type since the early Holocene (Kaal et al., 2011), even at the high precipitation rates experienced at our study site. Our results are in line with the well-documented oak dominance across the Muniellos reserve (Fernández Prieto and Sánchez, 1992) in the absence of any potential disruption of natural dynamics by management, either before the 1760s or after 1973 (Torrente, 2000, Alvarez, 2002). Furthermore, our results of past dynamics, successful recruitment, and current species composition together with the likely future increase in drought stress, suggest that oak will likely remain dominant under current and future conditions without human intervention (Clark et al., 2016).

Fire may also play an important role in maintaining the structure and species composition of oak forests (Abrams, 1992; Kaal et al., 2011; Bobiec et al., 2018). In Muniellos, we observed trees with deep, old fire scars, but we were not allowed to sample them because of conservation reasons. The open structure of our forest allows for the presence of light demanding, fire resilient shrub species (e.g. *Erica* sp). Low fire frequency favors oaks over shrubs (Pausas, 2006), while limiting shade-tolerant species, but increased fire frequencies would induce landscape changes from forest to shrublands (Kaal et al., 2011). Natural fires in temperate oak forests are generally low intensity, surface fires mainly affecting regeneration and not causing canopy tree mortality (Abrams, 1992). The lack of evidence of stand replacing disturbances over the last 500 years in our results and the lack of fire observational records in the reserve (Torrente, 2000, Alvarez, 2002) suggest that the role of fire at our study site could also mainly affect recruitment with little effects on canopy trees.

4.2. Forest growth and biomass retention

Forest biomass in Muniellos was dominated by large trees (DBH ≥ 70 cm), as has been commonly reported in temperate forests (Brown et al., 1997; Teets et al., 2018; Martin-Benito et al., 2020). In Muniellos, large trees represent around 50% of total AGB, exceeding values of 30% reported for old-growth forests with similar amounts of total AGB (Brown et al., 1997). In contrast, basal area and stem density were within the ranges reported for European mixed oak-beech (Petritan et al., 2012) and other old-growth forests (Burrascano et al., 2013), but higher than some oak-dominated forests in the southeastern United States (Hart et al., 2012).

Productivity of old-growth forests is usually lower than that of younger or secondary forests (Kutsch et al., 2009). Our estimated annual wood productivity of trees present at the time of sampling (~1.47 $Mg \cdot ha^{-1} \cdot year^{-1}$) was on the low end of temperate forests (Keeling and Phillips, 2007; Dye et al., 2016; Trotsiuk et al., 2016) but remained stable for the last few decades. Because mortality rates are unknown for the study forest, information about trees that died before the time of sampling and were not present in the forest in 2018 (so-called ghost trees) is not inherently present or obvious (Foster et al., 2014). Missing growth from ghost trees results in the underestimation of total AGB increment in the decades prior to sampling, although the effect is lower in old, slow growing forests (Foster et al., 2014). Our sampling of dead trees further reduces the AGBI underestimation due to ghost trees. In general, low productivity is expected from marginal sites, like our study forest, with shallow soils, high rock content and steep slopes. In fact, low productivity and difficult accessibility are probably the reasons why these stands were spared from logging (Stahle and Chaney, 1994). Similar annual productivities across our plots, despite differences in size and age structures, suggest that our productivity estimates may be representative for this landscape. In the most disturbed plots (MUN1 and MUN2), the disturbance in 1905–1915 likely resulted in the loss of a large part of their biomass but increased growth of remaining trees. Their lower current total AGB, but similar productivities, suggest that they may have not fully recovered their pre-disturbance AGB and may not be in a steady state.

The short-term growth decreases observed over the last 50 years could be attributed to different climate factors. Dominant and codominant trees, the largest contributors to stand-level growth, were sensitive to previous year precipitation and temperature, similar to other oak populations in the region (Rozas and García-González, 2012). Our climate-growth models suggest that low fall temperatures and abundant winter precipitation likely reduced stand growth in the mid 1970s and 1990s. In contrast, we suspect that the growth reduction peaking in 2017 was most probably due to spring-summer drought stress since 2015 combined with two late frosts in early May 2016 and late April 2017. Sporadic events of late spring frost and drought may induce sudden growth reductions in oak (Vitasse et al., 2019). Despite these periods of slow growth, the stand showed no long-term growth declines, a finding in line with evidence indicating no age-related growth declines (Kutsch et al., 2009; Xu et al., 2012; Foster et al., 2014). Beyond their many other ecosystem services (Wirth, 2009), these results further highlighting the importance of old-growth forests in terms of carbon fixation and storage.

Biomass accumulation over long periods of time leads to large amounts of carbon stored in forests (Luyssaert et al., 2008). Above ground biomass in our study forest (200–400 $Mg \cdot ha^{-1}$) was within the range of mature oak-dominated forests (Druckenbrod et al., 2005; Balboa-Murias et al., 2006; Saniga et al., 2014) and other temperate old-growth forests (Keeling and Phillips, 2007; Trotsiuk et al., 2016). The average biomass stocks and the low productivity observed in our plots resulted in long turnover times (153–229 years) compared to estimates for other temperate forests (Keeling and Phillips, 2007; Berner et al., 2017).

Our tree-ring based age estimations of AGB based on tree rings allowed for greater detail and precision on the analysis of biomass ages (system ages) in the forest. Mean carbon ages (MCA) ranged 108–167 years, which were lower than turnover times, but showed the same patterns between plots. Biomass stored in the forest longer than 100 years represented over 50% of total AGB in two plots, while at the landscape level, 13% of AGB (42 $Mg \cdot ha^{-1}$) was retained in the forest for >300 years (i.e., very old carbon). Thus, despite their low productivity, old-growth forests under stable forest conditions such as low disturbance rates with low synchrony in disturbance act as long-term carbon reservoirs. Increasing disturbances or harvesting in old-growth forests may release large amounts of stored carbon that would require centuries to recover (Pugh et al., 2019), as shown for our two most disturbed plots. Soils in old-growth forests also fix and store carbon longer than more disturbed forest (Knohl et al., 2003; Luyssaert et al., 2008), further increasing their carbon storage potential. These reservoirs are particularly important under the ongoing decrease of turnover times in forest carbon (Yu et al., 2019). Although old-growth forests in Europe represent less than 1% of the total forested area (Sabatini et al., 2018), temperate and boreal forest biomes represent 15% of forested area globally (FAO, 2006) and 10% of global net ecosystem productivity (Luyssaert et al., 2008). Long-term carbon storage capacity of old-growth forests plays a relevant role for the global carbon cycle (Luyssaert et al., 2008). Extending our tree-ring method to more precisely estimate AGB ages to a larger range of old-growth forests could contribute to a better understanding of their carbon storage potential in the context of climate change and increasing disturbances.

In single-compartment conceptual models like ours, where only AGB in wood is considered and wood is non-mobile between rings, turnover times and MCA should be identical (Sierra et al., 2017). However, the observed differences between turnover times and MCA at

the plot and stand levels suggest that the assumptions required for estimating turnover times as the ratios between AGB stock and AGB increments were not fully met. The estimation of turn-over times of forest carbon from empirical data likely introduces several sources of uncertainty. Our study forest may not be in a steady-state or near constant AGB stock, which would particularly affect plots MUN2 and MUN3 that may have not recovered their AGB stock after a larger disturbance in the early 1900s. Also, underestimation of AGB increments due to ghost trees (Foster et al., 2014) would result in an overestimation of turn-over times (Keith et al., 2009). Although mortality rates are unknown, releases since 1950 were more numerous than recruitment, which amounted to just a few new trees entering the forest per hectare (Fig. 3). Thus, AGB lost to mortality of a few trees large enough to leave a record in neighbouring trees likely exceeded AGB gains due to recruitment or to the faster growth of remaining trees because of the low productivity at the site. Yet, in our case the period considered for estimating AGB increments from tree rings (20–50 years) had little effect AGB increments and thus on turnover times.

Our dendrochronological approach to estimate MCA also presents several limitations. Uncertainty of the estimated AGB increments increases back in time because of decreasing sample sizes, missing parts of the cores not reaching the tree pith and ghost trees. This may be particularly important for large trees for which pith is not reached and for which past growth needs to be estimated from similar sized trees or for trees that grew fast at young ages and accumulated large AGB. This missing information results in underestimations of MCA by reducing the amount of AGB recovered in the earlier part of the chronology (Fig. 5). Sampling multiple cores from all trees would increase the probability of recovering more information of past growth and reduce this uncertainty. Uncertainty in MCA estimation would also be likely reduced in plots with much younger trees for which most of the past growth information can be recovered from tree cores. A wide scale study including similar sampling across a large range of forest with different ages, structures, species composition and disturbance dynamics could contribute to estimating the extent of these uncertainties. Better knowledge on the effect of stand dynamics and structure on mean carbon age and turnover times would contribute towards developing management practices that optimize carbon storage among other ecosystem services.

5. Conclusions

Our old-growth study forest appears to contain the oldest fully-documented, precisely-dated oak trees in the world. Under low disturbance regime, the forest experienced oak dominance and continuous recruitment for the last 500 years. If the conditions that led to the current day forest continue within similar ranges of variance over time, shade-tolerant species are unlikely to substitute oak as a dominant species in the near future. The absence of harvesting or large disturbances resulted in high forest stability and biomass accumulation, despite low forest productivity. The disturbance and growth dynamics that we documented resulted in carbon turnover times over a century and substantial amounts of biomass retained for longer than three centuries. Our results quantify the long periods of time that above ground woody biomass remains in old-growth and unmanaged forests and highlights their global role for carbon storage.

Supplementary data to this article can be found online at https://doi.org/10.1016/j.scitotenv.2020.142737.

CRediT authorship contribution statement

Dario Martin-Benito: Conceptualization, Methodology, Software, Formal analysis, Investigation, Data curation, Writing - original draft, Writing - review & editing, Visualization, Funding acquisition. **Neil Pederson:** Methodology, Investigation, Writing - review & editing. **Macarena Férriz:** Investigation, Writing - review & editing. **Guillermo Gea-Izquierdo:** Methodology, Investigation, Writing - review & editing, Funding acquisition.

Declaration of competing interest

The authors declare that they have no known competing financial interests or personal relationships that could have appeared to influence the work reported in this paper.

Acknowledgements

We are grateful to the *Consejería de Desarrollo Rural y Recursos Naturales* of the Principality of Asturias and the Fuentes del Narcea, Degaña e Ibias Natural Park for granting sampling permissions and specially to Antonio and Juan Carlos for their assistance in the field. We thank Enrique Garriga Garriga for processing cores samples and Lorenzo García Hermida for assistance with tree ring measurements. DMB was funded by projects AGL2015-73190-JIN and RYC-2017-23389, GGI by AGL2014-61175-JIN and RYC-2014-15864, and MF by FPI-SGIT2016-03 from the Spanish Ministry of Economy, Industry and Competitiveness. This is also a contribution to project PID2019-110273RB-I00 from the Spanish Ministry of Science and Innovation. The Spanish State Meteorological Agency (AEMET) contributed climate data to this study.

References

Abrams, M.D., 1992. Fire and the development of oak forests. Bioscience 346–353.
Abrams, M.D., Orwig, D.A., Dockry, M.J., 1997. Dendroecology and successional status of two contrasting old-growth oak forests in the Blue Ridge Mountains, U.S.A. Can. J. For. Res. 27, 994–1002.
Altman, J., Fibich, P., Dolezal, J., Aakala, T., 2014. TRADER: a package for tree ring analysis of disturbance events in R. Dendrochronologia 32, 107–112.
Altman, J., Fibich, P., Leps, J., Uemura, S., Hara, T., Dolezal, J., 2016. Linking spatiotemporal disturbance history with tree regeneration and diversity in an old-growth forest in northern Japan. Perspectives in Plant Ecology, Evolution and Systematics 21, 1–13.
Alvarez, J.L., 2002. La explotación del Monte de Muniellos (Asturias), 1766–1973. Ería 58, 273–286.
Annighofer, P., Beckschafer, P., Vor, T., Ammer, C., 2015. Regeneration patterns of European oak species (Quercus petraea (Matt.) Liebl., Quercus robur L.) in dependence of environment and neighborhood. PLoS ONE 10, e0134935.
Aranda, I., Gil, L., Pardos, J.A., 2000. Water relations and gas exchange in *Fagus sylvatica* L. and *Quercus petraea* (Mattuschka) Liebl. in a mixed stand at their southern limit of distribution in Europe. Trees - Structure and Function 14, 344–352.
Attiwill, P.M., 1994. The disturbance of forest ecosystems: the ecological basis for conservative management. For. Ecol. Manag. 63, 247–300.
Balboa-Murias, M.A., Rojo, A., Álvarez, J.G., Merino, A., 2006. Carbon and nutrient stocks in mature *Quercus robur* L. stands in NW Spain. Ann. For. Sci. 63, 557–565.
Berner, L.T., Law, B.E., Hudiburg, T.W., 2017. Water availability limits tree productivity, carbon stocks, and carbon residence time in mature forests across the western US. Biogeosciences 14, 365–378.
Bobiec, A., 2012. Białowieża primeval forest as a remnant of culturally modified ancient forest. Eur. J. For. Res. 131, 1269–1285.
Bobiec, A., Reif, A., Öllerer, K., 2018. Seeing the oakscape beyond the forest: a landscape approach to the oak regeneration in Europe. Landsc. Ecol. 33, 513–528.
Bormann, F.H., Likens, G.E., 1979. Pattern and Process in a Forested Ecosystem. Springer-Verlag, New York.
Bowman, D.M.J.S., Brienen, R.J.W., Gloor, E., Phillips, O.L., Prior, L.D., 2013. Detecting trends in tree growth: not so simple. Trends Plant Sci. 18, 11–17.
Brown, S., Schroeder, P., Birdsey, R., 1997. Aboveground biomass distribution of US eastern hardwood forests and the use of large trees as an indicator of forest development. For. Ecol. Manag. 96, 37–47.
Brzeziecki, B., Woods, K., Bolibok, L., Zajączkowski, J., Drozdowski, S., Bielak, K., Żybura, H., Leys, B., 2020. Over 80 years without major disturbance, late-successional Białowieża woodlands exhibit complex dynamism, with coherent compositional shifts towards true old-growth conditions. Journal of Ecology **doi** https://doi.org/10.1111/1365-2745.13367.
Bunn, A.G., 2008. A dendrochronology program library in R (dplR). Dendrochronologia 26, 115–124.
Burrascano, S., Keeton, W.S., Sabatini, F.M., Blasi, C., 2013. Commonality and variability in the structural attributes of moist temperate old-growth forests: a global review. For. Ecol. Manag. 291, 458–479.
Carbone, M.S., Czimczik, C.I., Keenan, T.F., Murakami, P.F., Pederson, N., Schaberg, P.G., Xu, X., Richardson, A.D., 2013. Age, allocation and availability of nonstructural carbon in mature red maple trees. New Phytol. 200, 1145–1155.
Carey, E.V., Sala, A., Keane, R., Callaway, R.M., 2001. Are old forests underestimated as global carbon sinks? Glob. Chang. Biol. 7, 339–344.
Castaño-Santamaría, J., Bravo, F., 2012. Variation in carbon concentration and basic density along stems of sessile oak (Quercus petraea (Matt.) Liebl.) and Pyrenean oak

(Quercus pyrenaica Willd.) in the Cantabrian Range (NW Spain). Ann. For. Sci. 69, 663–672.
Cavin, L., Mountford, E.P., Peterken, G.F., Jump, A.S., Whitehead, D., 2013. Extreme drought alters competitive dominance within and between tree species in a mixed forest stand. Funct. Ecol. 27, 1424–1435.
Cho, D.-S., Boerner, R.E.J., 1995. Dendrochronological analysis of the canopy history of two Ohio old-growth forests. Plant Ecol. 120, 173–183.
Cienciala, E., Apltauer, J., Exnerová, Z., Tatarinov, F., 2008. Biomass functions applicable to oak trees grown in Central-European forestry. J. For. Sci. 54, 109–120.
Clark, J.S., Iverson, L., Woodall, C.W., Allen, C.D., Bell, D.M., Bragg, D.C., D'Amato, A.W., Davis, F.W., Hersh, M.H., Ibanez, I., 2016. The impacts of increasing drought on forest dynamics, structure, and biodiversity in the United States. Glob. Chang. Biol. 22, 2329–2352.
Davis, S.C., Hessl, A.E., Scott, C.J., Adams, M.B., Thomas, R.B., 2009. Forest carbon sequestration changes in response to timber harvest. For. Ecol. Manag. 258, 2101–2109.
Di Filippo, A., Pederson, N., Baliva, M., Brunetti, M., Dinella, A., Kitamura, K., Knapp, H.D., Schirone, B., Piovesan, G., 2015. The longevity of broadleaf deciduous trees in Northern Hemisphere temperate forests: insights from tree-ring series. Front. Ecol. Evol. 3.
Díaz-Maroto, I.J., Vila-Lameiro, P., Vizoso-Arribe, O., Alañón, E., Díaz-Maroto, M.C., 2011. Natural forests of oak in NW Spain: soil fertility and main edaphic properties. In: Whalen, J.K. (Ed.), Soil Fertility Improvement and Integrated Nutrient Management: A Global Perspective. InTech, Rijeka, Croatiabrz, pp. 3–18.
Domínguez-Delmás, M., Rich, S., Traoré, M., Hajj, F., Poszwa, A., Akhmetzyanov, L., García-González, I., Groenendijk, P., 2020. Tree-ring chronologies, stable strontium isotopes and biochemical compounds: towards reference datasets to provenance Iberian shipwreck timbers. J. Archaeol. Sci. Rep. (in press).
Drobyshev, I., Gewehr, S., Berninger, F., Bergeron, Y., 2013. Species specific growth responses of black spruce and trembling aspen may enhance resilience of boreal forest to climate change. J. Ecol. 101, 231–242.
Druckenbrod, D.L., Shugart, H.H., Davies, I., 2005. Spatial pattern and process in forest stands within the Virginia piedmont. J. Veg. Sci. 16, 37–48.
Duncan, R.P., 1989. An evaluation of errors in tree age estimates based on increment cores in kahikatea (Dacrycarpus dacrydioides). New Zealand Natural Sciences 16, 1–37.
Dye, A., Barker Plotkin, A., Bishop, D., Pederson, N., Poulter, B., Hessl, A., 2016. Comparing tree-ring and permanent plot estimates of aboveground net primary production in three eastern US forests. Ecosphere 7, e01454.
European Environment Agency, 2006. European Forest Types. Categories and Types for Sustainable Forest Management Reporting and Policy. Technical Report No 9/2006. 9/2006. European Environment Agency.
FAO, 2006. Global forest resources assessment 2005: progress towards sustainable forest management. Food and Agriculture Organization of the United Nations. Italy, Rome.
Fernández Prieto, J.A., Sánchez, A.B., 1992. A new classification of the forests of the Muniellos Biological Reserve in Northwest Spain. Vegetatio 102, 33–46.
Foster, D.R., Orwlg, D.A., McLachlan, J.S., 1996. Ecological and conservation insights from reconstructive studies of temperate old-growth forests. Trends Ecol. Evol. 11, 419–424.
Foster, J., D'Amato, A., Bradford, J., 2014. Looking for age-related growth decline in natural forests: unexpected biomass patterns from tree rings and simulated mortality. Oecologia 175, 363–374.
Gea-Izquierdo, G., Cañellas, I., 2014. Local climate forces instability in long-term productivity of a Mediterranean oak along climatic gradients. Ecosystems 17, 228–241.
Gough, C.M., Curtis, P.S., Hardiman, B.S., Scheuermann, C.M., Bond-Lamberty, B., 2016. Disturbance, complexity, and succession of net ecosystem production in North America's temperate deciduous forests. Ecosphere 7, e01375.
Graumlich, L.J., Brubaker, L.B., Grier, C.C., 1989. Long-term trends in Forest net primary productivity: Cascade Mountains, Washington. Ecology 70, 405–410.
Hart, J.L., Clark, S.L., Torreano, S.J., Buchanan, M.L., 2012. Composition, structure, and dendroecology of an old-growth *Quercus* forest on the tablelands of the Cumberland Plateau, USAstah. For. Ecol. Manag. 266, 11–24.
Haylock, M.R., Hofstra, N., Klein Tank, A.M.G., Klok, E.J., Jones, P.D., New, M., 2008. A European daily high-resolution gridded data set of surface temperature and precipitation for 1950–2006. Journal of Geophysical Research: Atmospheres 113.
Heeter, K.J., Brosi, S.L., Brewer, G.L., 2019. Dendroecological analysis of xeric, upland, Quercus-dominated old-growth forest within the Ridge and Valley Province of Maryland, USA. Natural Areas Journal 39 (319–332), 314.
Holmes, R.L., 1983. Computer-assisted quality control in tree-ring dating and measurement. Tree-Ring Bull. 43, 69–78.
Jackson, T., Shenkin, A., Kalyan, B., Zionts, J., Calders, K., Origo, N., Disney, M., Burt, A., Raumonen, P., Malhi, Y., 2019. A new architectural perspective on wind damage in a natural forest. Frontiers in Forests and Global Change 1, 1–13.
Kaal, J., Carrión Marco, Y., Asouti, E., Martín Seijo, M., Martínez Cortizas, A., Costa Casáis, M., Criado Boado, F., 2011. Long-term deforestation in NW Spain: linking the Holocene fire history to vegetation change and human activities. Quat. Sci. Rev. 30, 161–175.
Keeling, H.C., Phillips, O.L., 2007. The global relationship between forest productivity and biomass. Glob. Ecol. Biogeogr. 16, 618–631.
Keith, H., Mackey, B.G., Lindenmayer, D.B., 2009. Re-evaluation of forest biomass carbon stocks and lessons from the world's most carbon-dense forests. Proc. Natl. Acad. Sci. U. S. A. 106, 11635–11640.
Klesse, S., Etzold, S., Frank, D., 2016. Integrating tree-ring and inventory-based measurements of aboveground biomass growth: research opportunities and carbon cycle consequences from a large snow breakage event in the Swiss Alps. Eur. J. For. Res. 135, 297–311.
Knohl, A., Schulze, E.-D., Kolle, O., Buchmann, N., 2003. Large carbon uptake by an unmanaged 250-year-old deciduous forest in Central Germany. Agric. For. Meteorol. 118, 151–167.
Kutsch, W.L., Wirth, C., Kattge, J., Nöllert, S., Herbst, M., Kappen, L., 2009. Ecophysiological characteristics of mature trees and stands-consequences for old-growth forest productivity. Old-growth Forests. Springer, pp. 57–79.
Lorimer, C., Frelich, L., 1989. A methodology for estimating canopy distubance frequency and intensity in dense temperate forest. Can. J. For. Res. 19, 651–663.
Luyssaert, S., Schulze, E.D., Börner, A., Knohl, A., Hessenmöller, D., Law, B.E., Ciais, P., Grace, J., 2008. Old-growth forests as global carbon sinks. Nature 455, 213–215.
Manion, P.D., 1981. Tree Disease Concepts. Prentice-Hall, Inc., Englewood Cliffs, New Jersey.
Manrique González, J.M., Oviedo, F. Bravo, del Peso Taranco, C., de Aza, C. Herrero, 2017. Ecuaciones de biomasa para roble albar (*Quercus petraea* (Matt.) Liebl.) y rebollo (*Quercus pyrenaica* Willd) en la comarca de la "Castillería" en el Norte de la Provincia de Palencia.*in* VII Congreso Forestal Español.
Martin-Benito, D., Pederson, N., Lanter, C., Köse, N., Doğan, M., Bugmann, H., Bigler, C., 2020. Disturbances and climate drive structure, stability, and growth in mixed temperate old-growth rainforests in the Caucasus. Ecosystems 23, 1170–1185.
Masaki, T., Tanaka, H., Tanouchi, H., Sakai, T., Nakashizuka, T., 1999. Structure, dynamics and disturbance regime of temperate broad-leaved forests in Japan. J. Veg. Sci. 10, 805–814.
McEwan, R.W., Dyer, J.M., Pederson, N., 2011. Multiple interacting ecosystem drivers: toward an encompassing hypothesis of oak forest dynamics across eastern North America. Ecography 34, 244–256.
McEwan, R.W., Pederson, N., Cooper, A., Taylor, J., Watts, R., Hruska, A., 2014. Fire and gap dynamics over 300 years in an old-growth temperate forest. Appl. Veg. Sci. 17, 312–322.
Oliver, C.D., Larson, B.C., 1996. Forest Stand Dynamics. updated edition. Wiley, New York.
Pausas, J.G., 2006. Simulating Mediterranean landscape pattern and vegetation dynamics under different fire regimes. Plant Ecol. 187, 249–259.
Pederson, N., 2010. External characteristics of old trees in the eastern deciduous forest. Nat. Areas J. 30, 396–407.
Petritan, A.M., Biris, I.A., Merce, O., Turcu, D.O., Petritan, I.C., 2012. Structure and diversity of a natural temperate sessile oak (Quercus petraea L.) – European beech (Fagus sylvatica L.) forest. For. Ecol. Manag. 280, 140–149.
Petritan, A.M., Bouriaud, O., Frank, D.C., Petritan, I.C., 2017. Dendroecological reconstruction of disturbance history of an old-growth mixed sessile oak–beech forest. J. Veg. Sci. 28, 117–127.
Pinheiro, J., Bates, D., DebRoy, S., Sarkar, D., R. C. Team, 2019. nlme: Linear and Nonlinear Mixed Effects Models. R Package Version 3.1–14. https://cran.r-project.org/package=nlme.
Piovesan, G., Biondi, F., Baliva, M., De Vivo, G., Marchianò, V., Schettino, A., Di Filippo, A., 2019. Lessons from the wild: slow but increasing long-term growth allows for maximum longevity in European beech. Ecology 100, e02737.
Piovesan, G., Baliva, M., Calcagnile, L., D'Elia, M., Dorado-Linan, I., Palli, J., Siclari, A., Quarta, G., 2020. Radiocarbon dating of Aspromonte sessile oaks reveals the oldest dated temperate flowering tree in the world. Ecology, e03179.
Pretzsch, H. 2009. Forest dynamics, growth, and yield. Pages 1-39 Forest dynamics, growth and yield. Springer.
Pugh, T.A.M., Arneth, A., Kautz, M., Poulter, B., Smith, B., 2019. Important role of forest disturbances in the global biomass turnover and carbon sinks. Nat. Geosci. 12, 730–735.
R Core Team, 2019. R: A Language and Environment for Statistical Computing. R Foundation for Statistical Computing, Vienna, Austria http://www.r-project.org/.
Ranius, T., Niklasson, M., Berg, N., 2009. A comparison of methods for estimating the age of hollow oaks. Ecoscience 16, 167–174.
Rinn, F., 2003. TSAP-Win Professional, Time Series Analysis and Presentation for Dendrochronology and Related Applications. Version 0.3, Quick Reference. Frank Rinn, Heidelberg, Germany.
Rodríguez-Calcerrada, J., Pardos, J.A., Gil, L., Reich, P.B., Aranda, I., 2008. Light response in seedlings of a temperate (*Quercus petraea*) and a sub-Mediterranean species (*Quercus pyrenaica*): contrasting ecological strategies as potential keys to regeneration performance in mixed marginal populations. Plant Ecol. 195, 273–285.
Rozas, V., 2004. A dendroecological reconstruction of age structure and past management in an old-growth pollarded parkland in northern Spain. For. Ecol. Manag. 195, 205–219.
Rozas, V., 2005. Dendrochronology of pedunculate oak (*Quercus robur* L.) in an old-growth pollarded woodland in northern Spain: tree-ring growth responses to climate. Ann. For. Sci. 62, 209–218.
Rozas, V., García-González, I., 2012. Too wet for oaks? Inter-tree competition and recent persistent wetness predispose oaks to rainfall-induced dieback in Atlantic rainy forest. Global and Planetary Change 94-95, 62–71.
Ruffner, C.M., Abrams, M.D., 1998. Relating land-use history and climate to the dendroecology of a 326-year-old Quercus prinus talus slope forest. Can. J. For. Res. 28, 347–358.
Runkle, J.R., 1985. Disturbance regimes in temperate forests. In: Pickett, S., White, P.S. (Eds.), The Ecology of Natural Disturbance and Patch Dynamics. Academic Press, San Diego, pp. 17–33.
Sabatini, F., Jiménez-Alfaro, B., Burrascano, S., Blasi, C., 2014. Drivers of herb-layer species diversity in two unmanaged temperate forests in northern Spain. Community Ecology 15, 147–157.
Sabatini, F.M., Burrascano, S., Keeton, W.S., Levers, C., Lindner, M., Pötzschner, F., Verkerk, P.J., Bauhus, J., Buchwald, E., Chaskovsky, O., Debaive, N., Horváth, F., Garbarino, M., Grigoriadis, N., Lombardi, F., Marques Duarte, I., Meyer, P., Midteng, R., Mikac, S., Mikoláš, M., Motta, R., Mozgeris, G., Nunes, L., Panayotov, M., Ódor, P., Ruete, A., Simovski, B., Stillhard, J., Svoboda, M., Szwagrzyk, J., Tikkanen, O.-P., Volosyanchuk, R., Vrska, T., Zlatanov, T., Kuemmerle, T., Essl, F., 2018. Where are Europe's last primary forests? Diversity and Distributions 24, 1426–1439.

Saniga, M., M. Balanda, S. Kucbel, and J. Pittner. 2014. Four decades of forest succession in the oak-dominated forest reserves in Slovakia. iForest-Biogeosciences and Forestry **7**:324.

Seidl, R., Thom, D., Katz, M., Martin-Benito, D., Peltoniemi, M., Vacchiano, G., Wild, J., Ascoli, D., Petr, M., Honkaniemi, J., Lexer, M.J., Trotsiuk, V., Mairota, P., Svoboda, M., Fabrika, M., Nagel, T.A., Reyer, C.P.O., 2017. Forest disturbances under climate change. Nature Climate Change 7, 395–402.

Sierra, C.A., Müller, M., Metzler, H., Manzoni, S., Trumbore, S.E., 2017. The muddle of ages, turnover, transit, and residence times in the carbon cycle. Global Change Biology 23, 1763–1773.

Souto-Herrero, M., Rozas, V., García-González, I., 2017. A 481-year chronology of oak earlywood vessels as an age-independent climatic proxy in NW Iberia. Global and Planetary Change. 155, 20–28.

Sperduto, D. D., W. F. Nichols, K. F. Crowley, and D. A. Bechtel. 2000. Black Gum (*Nyssa sylvatica* Marsh.) in New Hampshire. New Hampshire Natural Heritage Inventory, Concord, Concord, NH.

Stahle, D.W., Chaney, P.L., 1994. A Predictive Model for the Location of Ancient Forests. Natural Areas Journal 14, 151–158.

Stahle, D.W., Griffin, R.D., Meko, D.M., Therrell, M.D., Edmondson, J.R., Cleaveland, M.K., Stahle, L.N., Burnette, D.J., Abatzoglou, J.T., Redmond, K.T., Dettinger, M.D., Cayan, D.R., 2013. The Ancient Blue Oak Woodlands of California: Longevity and Hydroclimatic History. Earth Interactions 17, 1–23.

Teets, A., Fraver, S., Weiskittel, A.R., Hollinger, D.Y., 2018. Quantifying climate–growth relationships at the stand level in a mature mixed-species conifer forest. Global Change Biology 24, 3587–3602.

Torrente, J. P. 2000. The Muniellos Forests (Asturias, Spain) in history. Forest history: international studies on socio-economic and forest ecosystem change. Report No. 2 of the IUFRO Task Force on Environmental Change.:119–126.

Trotsiuk, V., Svoboda, M., Weber, P., Pederson, N., Klesse, S., Janda, P., Martin-Benito, D., Mikolas, M., Seedre, M., Bace, R., Mateju, L., Frank, D., 2016. The legacy of disturbance on individual tree and stand-level aboveground biomass accumulation and stocks in primary mountain *Picea abies* forests. Forest Ecology and Management 373, 108–115.

Vallet, P., Dhôte, J.-F., Moguédec, G.L., Ravart, M., Pignard, G., 2006. Development of total aboveground volume equations for seven important forest tree species in France. Forest Ecology and Management 229, 98–110.

Vicente-Serrano, S.M., Beguería, S., López-Moreno, J.I., 2010. A multiscalar drought index sensitive to global warming: the standardized precipitation evapotranspiration index. Journal of Climate 23, 1696–1718.

Vitasse, Y., Bottero, A., Cailleret, M., Bigler, C., Fonti, P., Gessler, A., Levesque, M., Rohner, B., Weber, P., Rigling, A., Wohlgemuth, T., 2019. Contrasting resistance and resilience to extreme drought and late spring frost in five major European tree species. Global Change Biology 25, 3781–3792.

Wirth, C., 2009. Old-Growth Forests: Function, Fate and Value – a Synthesis. Pages 465–491 *in* Springer, editor. Berlin, Heidelberg, Old-growth forests.

Xu, C.-Y., Turnbull, M.H., Tissue, D.T., Lewis, J.D., Carson, R., Schuster, W.S.F., Whitehead, D., Walcroft, A.S., Li, J., Griffin, K.L., 2012. Age-related decline of stand biomass accumulation is primarily due to mortality and not to reduction in NPP associated with individual tree physiology, tree growth or stand structure in a Quercus-dominated forest. Journal of Ecology 100, 428–440.

Xu, K., Wang, X., Liang, P., Wu, Y., An, H., Sun, H., Wu, P., Wu, X., Li, Q., Guo, X., Wen, X., Han, W., Liu, C., Fan, D., 2019. A new tree-ring sampling method to estimate forest productivity and its temporal variation accurately in natural forests. Forest Ecology and Management 433, 217–227.

Yu, K., Smith, W.K., Trugman, A.T., Condit, R., Hubbell, S.P., Sardans, J., Peng, C., Zhu, K., Peñuelas, J., Cailleret, M., Levanic, T., Gessler, A., Schaub, M., Ferretti, M., Anderegg, W.R.L., 2019. Pervasive decreases in living vegetation carbon turnover time across forest climate zones. Proceedings of the National Academy of Sciences 116, 24662–24,667.